ANL/LWR/SAF--84-1

DE84 013937

HYDRODYNAMIC SWEEPOUT THRESHOLDS IN BWR MARK III REACTOR CAVITY INTERACTIONS

by

B. W. Spencer, S. P. Baronowsky, and D. J. Kilsdonk

April 1984

Argonne National Laboratory
9700 South Cass Avenue
Argonne, Illinois 60439

Prepared for:
Atomic Industrial Forum
Industry Degraded Core Rulemaking (IDCOR) Program
Technology for Energy Corporation
Knoxville, Tennessee 37922
E. L. Fuller, TEC, Program Manager
R. E. Henry, FAI, Technical Coordinator

This work was carried out at Argonne National Laboratory which is operated for the U. S. Department of Energy under Contract W-31-109-Eng-38.

TABLE OF CONTENTS

LIST OF FIGURES

LIST OF TABLES

HYDRODYNAMIC SWEEPOUT THRESHOLDS IN BWR MARK III REACTOR CAVITY INTERACTIONS

by

B. W. Spencer, S. P. Baronowsky, and D. J. Kilsdonk

EXECUTIVE SUMMARY

Simulant-material experiments and related analysis are described which investigated hydrodynamics aspects of ex-vessel interactions following postulated core meltdown with subsequent meltthrough of the vessel lower head and ejection of molten corium from the vessel into the containment region beneath the vessel. The specific containment design investigated here is a BWR Mark III in which there is a deep concrete-lined cavity (pedestal region) beneath the RPV. The principal objectives of the investigation were to examine the possible sweepout of water and corium from the cavity by action of the steam/H_2 flow through the system (originating primarily from vessel blowdown and augmented by corium/water thermal interaction) and to model the sweepout process for application to the full-size reactor system. The dispersal pathways in this containment design include a single manway and four CRD penetrations in the cylindrical pedestal wall connecting to the drywell with a combined cross-sectional area of ~ 10 m^2. These openings range from 3.4 to 6.3 m in elevation off the concrete floor of the cavity.

The experiments were performed using a 1:34 scale mock-up of the RPV/pedestal region. The first tests were quasi-steady tests in which the gas flowrate through the system was gradually increased to determine the flowrate at incipient sweepout using water in the cavity. Tests were also performed using molten Wood's metal (WM) to represent the corium, ejected into the mock-up at varying pressure and varying rates of follow-on gas flowrate to represent the vessel blowdown. Some tests were performed with water on the cavity floor, and one test was performed using steel shot to repreent a fragmented debris bed. The tests were photographed using high speed motion pictures.

The test results indicated that threshold gas flowrates existed beyond which dispersal of water and/or corium from the cavity can be expected. The predominant dispersal flow regime observed in the experiments involved fluidization of the water or molten WM by the gas flowrate through the system and sweepout of the fluidized liquid droplets as the gas exited the cavity through the openings in the wall. The superficial gas velocity at the onset of water sweepout ranged from 0.87 to 1.04 m/s in the tests which agrees very closely to the calculated fluidization threshold of 0.96 m/s. Application of the fluidization model for prediction of sweepout for the full-size system suggests that sweepout of water and corium can occur if the breach size in the RPV lower head exceeds ~ 10 and 17 cm diameter, respectively, for steam blowdown at a vessel initial pressure of 1000 psi.

I. INTRODUCTION

A. Background

This is the third in a series of reports on investigations of the dispersion of corium debris from the reactor cavity to other parts of the reactor containment building (RCB) for postulated core-melt accident sequences involving vessel meltthru. Previous studies have investigated corium dispersiveness for a Zion-type PWR containment design.[1,2] The present investigation deals with a containment design representative of the Grand Gulf BWR system (Mark III containment). In these investigations it is postulated as an initial condition that core uncovery occurs, core materials melt forming "corium," the corium eventually drains to the bottom head of the reactor pressure vessel (RPV), and the vessel head fails locally (at penetration weldments) due to corium-to-steel heat transfer. Vessel failure would initiate release of the molten corium into the region of the containment building beneath the RPV, i.e., the reactor cavity or pedestal region. The conditions of this release are scenario dependent, namely the RPV pressure which drives the corium efflux, the corium melt mass available to be ejected from the RPV, the ejection flow regime (possibly involving 2ϕ effects due to flashing of dissolved or trapped gas and gas breakthru at the top surface of the melt layer), and the breach area. The conditions in the pedestal region where the corium enters are design specific, namely the local volume, the pathway area and geometry connecting the pedestal volume to the drywell and/or suppression pool, and the presence or absence of water on the pedestal floor.

The overall objective of these studies is to assess under what conditions the corium which enters the pedestal region may be retained in that region or may be further dispersed through available pathways into other parts of the containment. Corium which is not dispersed elsewhere accumulates primarily on the floor as a melt layer or debris bed, and subsequent attack on the concrete surfaces may be expected. This is expected to be the case particularly for low RPV pressure and dry cavity. If the RPV pressure is high or if water is present on the pedestal floor, the blowdown gas/steam mixture, perhaps augmented by steam generated in the pedestal by corium/water thermal interaction, will flow from the pedestal volume through available openings into the surrounding drywell volume. If this gas/steam flowrate is sufficiently large,

corium may be entrained into the flow stream and may be dispersed from the pedestal volume by action of this high-velocity stream. The significance of this is that debris may be distributed to other parts of the containment volume than the pedestal region, lessening the mass available on the pedestal floor. This eases debris coolability requirements if water is available in the cavity, and lessens attack on concrete and structure if water is not available. On the negative side, if dispersed corium is not quenched by contact with water it may cause some degree of direct heatup of the containment atmosphere and may cause undesirable heatup of surfaces such as equipment, concrete, and penetration seals in the drywell volume.

B. Objective

The general objective of this study was to investigate entrainment and sweepout phenomena for a cavity configuration representing the Grand Gulf Mark III containment design. The specific objectives were:

1) To visually observe the hydrodynamic processes associated with vessel blowdown and/or rapid steam generation in the reactor pedestal region;

2) To determine the threshold gas flowrates through the system at which entrainment and sweepout become significant for i) water preexisting in the cavity, ii) a particle bed preexisting in the cavity, and iii) a high-density corium-simulant injected into the cavity; and

3) To assess the entrainment and sweepout behavior in terms of analytical models in order to extrapolate the behavior observed in scale-model, separate-effects tests to the reactor system.

C. Approach

A series of scale-model, simulant-material tests was undertaken to examine the hydrodynamic phenomena. These were "separate-effects" tests in the sense that phenomena other than hydrodynamic phenomena would be encountered in the reactor system, namely steam generation and other heating effects of corium quench, oxidation of constituents of the corium (energy and H_2 release),

corium attack on the concrete surfaces (gas release, aerosol production), among others. However, for the purposes of satisfying test objectives, i.e., to examine and model the entrainment/dispersal thresholds associated with vessel blowdown into the cavity, the governing phenomena were hydrodynamic rather than heat transfer related. Heat transfer effects could augment the flowrate from vessel blowdown by producing steam and gasses in the cavity, contributing to the overall gas flowrate exiting the cavity region. In the hydrodynamic experiments, this is lumped together with the blowdown gas, wherein the gas flowrate used in the experiments may be regarded as analogous to gas/steam flowrate from all sources in the reactor system.

The experiment apparatus was constructed of transparent Plexiglas so that the entrainment and dispersal behavior could be observed using high-speed motion pictures. The apparatus was a scale mock-up containing the essential compartments and interconnecting pathways based on the Grand Gulf Mark III BWR containment design (Fig. 1). Two types of tests were run. In order to obtain data for the sweepout threshold, the first series of tests was performed in a quasi-static manner in which the fluid or particle bed preexisted on the base of the apparatus, and the gas flowrate was gradually increased until significant sweepout was observed for the various materials of interest. The second series of tests depicted the accident sequence more closely. In order to visualize the hydrodynamic processes of corium *injected* into the cavity, a mass of high-density, molten corium simulant was injected into the cavity. The follow-on gas flowrate was held approximately constant at magnitudes both above and below the sweepout threshold for comparisons. The sweepout threshold data was compared with existing fluidization models.

II. EXPERIMENT DESCRIPTION

A. Apparatus

The mock-up of the Grand Gulf Mark III cavity constructed for the tests is shown in Figs. 2a and 2b. The mock-up consists of four principal components, namely: i) the cavity section, ii) the weir wall section, iii) the vessel mock-up (injector), and iv) the gas flow system. The apparatus is constructed of transparent Plexiglas to approximately 1:34 linear scale based upon the Grand Gulf containment.[3] The weir wall section is present in the apparatus primarily to contain the dispersed debris. No attempt was made to make this section an exact geometric replica.

The Grand Gulf containment is shown in Fig. 1. The cavity region consists of the RPV pedestal and the weir wall. The RPV pedestal is formed from reinforced concrete in a vertical cylinder of 9.3 m height with a constant outside diameter of ~ 10 m. The inside diameter varies from 6.5 m to 5.7 m. The pedestal is rigidly connected to a circular, reinforced concrete basemat of 20.7 m diameter with a thickness of 2.4 m. The reactor pressure vessel (RPV) is connected to the pedestal by 120 high-strength bolts of 8.9 cm diameter.

The five major penetrations through the pedestal consist of four control rod drive (CRD) supports and an access port. These penetrations provide the major area for removal of the debris from the cavity. The CRD penetrations are 1.7 m x 1.2 m openings loca ed 6.25 m above the containment floor. The access port is a 0.9 m x 2.1 m opening located 3.4 m above the containment floor.

In the experiment apparatus, Fig. 2, the inner diameter change is obtained by the insertion of an inner ring of transparent Plexiglas fabricated according to model scale. The penetrations were located on the model, and the openings shown in Fig. 2 were cut through the Plexiglas wall. The weir wall section is located at the scale radial distance from the cavity opening although not fabricated to a scale height. A porous grid plate was placed atop the apparatus to allow blowdown gas to escape upward while still retaining most of the water and Wood's metal (WM) in the annulus for subsequent measurement. A closeup of the cavity apparatus is shown in Fig. 3.

The WM injector is illustrated in Fig. 2a. The injector has a working volume of 214 cm^3. It was outfitted with heaters and thermal insulation in order to heat the WM to the desired initial temperature. The mass of WM used for the tests was 2 kg. This amount represents ~ 78,600 kg of corium which represents approximately 13% of the total core mass. To initiate ejection of the WM, the injector was pressurized to the failure point of the rupture disk. For the tests that required a rupture disk, two 1-mil aluminum rupture disks were used. These disks ruptured consistently at an injector pressure of 0.20 MPa. The material exited through a 2.54 cm ID nozzle. A closeup of the injector mounted on the cavity apparatus is shown in Fig. 4.

The gas system is illustrated in Fig. 5. The system consisted of a manifold of nitrogen bottles, pressure regulators, flow control valves, and an instrumented manifold using orifice plates to measure the gas flowrate. For these tests, only the 1-inch manifold line was used with the orifice throat diameter, D_t-1, of 1.7 cm. Flow was initiated using the solenoid-operated safety valve. For the quasi-static dispersal threshold tests, flow was controlled with the lever-operated ball valve on the main gas line.

B. Instrumentation

In addition to the orifice and temperature mesurements in the gas line used to determine the gas flow conditions, instrumentation consisted of strain gauge type pressure sensors in the injector and cavity to measure injection pressure and cavity pressurization, respectively, plus thermocouples located in the injector and cavity to measure WM temperature and cavity ambient temperature, respectively. The injector PT (PT-1) was an Alinco Model 151, 0-300 psig range, S/N 25290; the cavity PT (PT-2) was a Data Sensors Model PB4143B-13, ± 25 psid range, S/N 108. The PT across the orifice on the gas flow line was Statham Model PM 399 TC, ± 50 psid range, S/N 93; the PT on the downstream side of the orifice was a Dynisco Model PT182, 0-300 psig range, S/N 30961. The pressure sensors were calibrated using a deadweight tester and technique traceable to NBS standards. The data was recorded on a Honeywell Model 1858 fibre-optics recorder using Model 1887A amplifier modules.

The principal diagnostics for these dispersal phenomena experiments were the motion pictures. A HYCAM high-speed camera was used. The camera speed

was 500 fps for the quasi-static tests and 1000 fps for the dynamic tests. Ektachrome 7241 and 7251 film was used.

C. Experiment Procedure

For the tests that used Wood's metal, the metal was melted in a separate heating apparatus, and a measured mass was loaded into the preheated injector. The melt temperature was typically 90C. Water used in the cavity was dyed red for enhanced visibility in the motion pictures, and the cavity was filled to the desired initial level. The pressure regulators and flowrate controls were set to the desired conditions. The diffusers for the backlighting, the lighting, and camera were positioned according to a preestablished and consistent arrangement. The instrumentation calibrations were checked, and calibrated signals were recorded for reference on the visicorder. When the pretest preparations were completed, the lighting, camera, and recorder were switched on.

For the quasi-static dispersal threshold tests, the solenoid activated safety valve was opened, and gas flow was controlled by slowly opening the lever-operated ball valve on the main gas line. The dynamic transient tests were controlled by pressurizing the gas line up to the solenoid valve and triggering the solenoid with an auto sequence timer. This pressurized the injector, bursting the rupture disk, and expelling the injection material.

Following the tests, the remaining water was drained and the WM dried using heat lamps. The debris was removed from specified zones and weighed. The motion pictures as well as test data were examined for characteristic threshold velocities and debris dispersion.

III. EXPERIMENT RESULTS

A list of the eight tests performed in this series is given in Table 1. The quasi-static dispersal threshold tests and dynamic transient tests are denoted by S and D, resepctively. Tests #1 and #2 were quasi-static tests to determine the minimum gas flowrate required to entrain and disperse water droplets for this geometry. The gas flowrate ranged from 0 to 0.26 kg/s for test #1 and from 0 to 0.20 kg/s for test #2. Test #3 was another quasi-static test with a lower gas flowrate range, from 0 to 0.07 kg/s. Test #4 was a dynamic transient test with a gas flow of ~ 0.05 kg/s applied. The removal of water from the cavity under sustained gas flow was analyzed in this test. Test #5 was a dynamic transient simulant corium/water cavity interaction with Wood's metal injected into water with sustained gas flow of ~ 0.05 kg/s following. Test #6 was a dynamic transient test with gas flowing over a simulant fragment bed. The bed consisted of steel shot of ~ 780 μm diameter representing a fragmented bed of corium with a porosity of ~ 0.50. The volume of shot was calculated, assuming a dry bed, to be ~ 421 cm^3. Tests #7 and #8 were dynamic transient tests with WM injected into a dry cavity and water, respectively. Sustained gas flow of ~ 0.25 kg/s followed.

A. Threshold Tests

Tests #1-3 were quasi-static tests of gas flowing onto a layer of water on the floor of the cavity. The gas flowrate was slowly increased to determine the onset of droplet entrainment and removal from the floor. Tests #1 and #2 were performed without the CRD openings in the apparatus. Test #3 and all subsequent tests were performed with the CRD ports. Entrainment in Tests #1 and #2 began at a gas flowrate of ~ 0.025 kg/s. Adding the CRD openings in test #3 increased the required entrainment threshold flowrate to ~ 0.030 kg/s. Test #2 was performed with half the water level as in test #1 and the threshold flowrate was found to be independent of the water height.

B. Transient Tests

Test #4 was the first dynamic transient test. The gas flowrate was set at a constant rate of ~ 0.048 kg/s such that the threshold for water entrain-

Table 1. Summary of Cavity Interaction Tests - Grand Gulf Series

Test Number (Type) (Old Ref.)	1(S) (23A)	2(S) (23B)	3(S) (29A)	4(D) (29B)	5(D) (30)	6(D) (31)	7(D) (32)	8(D) (33)
Injected material[1]	gas	gas	gas	gas	WM/gas	gas	WM/gas	WM/gas
Cavity material	water	water	water	water	water	steel shot	none	water
Cavity material level, V/V_T[2]	.20	.10	.20	.20	.20	.06	-	.20
Injector temperature, C	26	26	26	26	91	27	91	91
Injection pressure, MPa g	-[3]	-	-	-	.2	.2	.375	.325
WM injection velocity, m/s	-	-	-	-	3.79	-	4.44	4.28
Gas flowrates:								
a) Range for Dispersal threshold tests, kg/s	0-.256	0-.200	0-.073	-	-	.052-.132	-	-
b) Threshold velocity for onset of dispersion, kg/s	.025	.025	.030	-	>0.54	.088	<.25	<.25
c) Flowrate for dynamic tests, kg/s	-	-	-	.048	.054	-	.25	.25

S = Quasi-static pressurization

D = Dynamic transient

(1) WM = Wood's Metal (T_{mp} = 73C)

(2) V_T = Total cavity volume, 7306 cm^3

(3) Negligible pressurization

ment and dispersal was surpassed by a small margin. Figures 6a and 6b are selected frames from the motion picture films of this test. Impact of the gas jet on the surface of the water formed a crater and surrounding wave which propagated radially from the point of incidence to the wall. The crater penetrated to the cavity floor and expanded radially outward. At this time, t = 150 ms, the remaining water is mixed with the gas into a turbulent two-phase regime. The two-phase mixture then "boils up" and fills the cavity. Up to this time, the water that exited from the cavity was sloshed out by the waves formed by the impacting gas jet. The two-phase mixture then exits the openings, t = 240 ms, as a two-phase jet and impacts on the weir wall. As the water is removed, the void fraction in the exiting jet increases and eventually becomes a fine droplet dispersed regime. The remaining water in the cavity flows along the cavity walls as a thin film. Further removal of water is by entrainment of droplets from the water film, t > 3600 ms. The cavity is essentially emptied by t = 6000 ms.

Test #5 was a dynamic transient test with Wood's metal injected into water. The gas flowrate was set greater than the dispersal threshold flowrate for water and less than the dispersal threshold flowrate for WM. Figures 7a and 7b show selected motion picture frames for this test. The initial impact of the WM, Fig. 7a, t = 70 ms, formed a radially symmetric crater-like mixing region. The impact formed a wave on the water surface that spread radially outward. As the mixing region penetrated the water layer, the displaced water formed an annular-type geometry that rose along the cavity wall. The gas flowrate was initiated at approximately 100 ms when the gas broke through the WM trailing edge. At the onset of gas flow, the water splash wave had already risen to occlude the CRD access port opening. Some of the water-WM mixture was immediately swept out of the opening. The WM predominantly settled to the cavity floor, however, and formed a pool. Very little WM was removed from the cavity except that which had been dispersed in the swept-out water. Posttest photos, Figs. 8 and 9, show the WM collected on the floor of the cavity including the crater in the central region where the gas jet impacted on the base. Some WM formed a thin crust on the cavity wall as it was carried up with the water. Figure 8 shows a crust of WM on the weir wall from the impact of the WM/water/gas jet exiting the CRD ports. The impact of the mixture on the weir wall formed a rising film on the weir wall surface that exited through the porous plate as can be seen in Fig. 8.

The results of test #5 showed that the gas flowrate was sufficient to cause dispersal of the water, but that dispersal of WM was small and was attributable to a wave splashing mechanism rather than by sustained levitation and sweepout. The water carried some WM up the cavity wall, but the WM solidified forming a crust. Figure 9 shows that the WM was quenched into irregular-shaped fragments which collected on the base together with an unquenched melt layer.

Test #6 was a dynamic transient test with a slowly increasing gas flowrate. The cavity material was steel shot having a volume of ~ 421 cm^3. The shot diameter was uniform at 780 μm. The shot represented a particle bed of fragmented corium at 50% theoretical density. Figures 10a and 10b are selected motion picture frames from test #6. The impact of the gas jet on the bed propelled the shot radially against the cavity wall. The shot was levitated on the wall in an annular fashion. When the shot reached the first opening, the CRD access port, it was swept out with the gas. Subsequently, the shot was uniformly levitated throughout the entire cavity volume (except for the jet) and was slowly swept out by the gas leaving the cavity through the openings. From analysis of the data, the threshold flowrate to levitate, entrain, and sweepout the shot was ~ 0.088 kg/s.

Test #7 was a dynamic transient test injecting WM into a dry cavity with a constant gas flowrate of ~ 0.25 kg/s following, chosen to far surpass the sweepout threshold for the WM. Figures 11a and 11b are selected frames from the motion picture of this test. The initial fragmenting of the leading edge of the WM stream was due to the bursting of the rupture disk. The gas flowrate follows at t = 35 ms by breaking through the trailing edge of the WM column. Some WM was immediately entrained by the breakthrough gas and was swept out through the CRD port openings. Most of the WM splashed off the base and was levitated as a liquid film on the cavity wall. The liquid film was subsequently "ripped" off the wall and entrained into the upward flowing gas. The entrained WM then exited the cavity and impacts on the weir wall where it forms a film on the weir wall. By t = 900 ms, the cavity is essentially cleared of the WM except for a thin frozen crust on the wall and on the floor. The WM is dispersed throughout the weir wall and along the top porous plate.

Test #8 was similar to test #7 except that there was water on the cavity base. The gas flowrate was greater than the sweepout threshold for both water and WM. The WM was removed from the cavity as was all of the water. The gas flow caused effective intermixing of the WM and water. The WM fragmented and froze into small particles in this test. The WM/water mixture was swept out of the cavity opening in a similar fashion as in the previous tests. Figure 12 is a posttest photo of that cavity apparatus showing that the cavity was essentially emptied of all water and WM. The photo also shows the crust on the cavity walls and the weir wall assembly. This crust is typical of those found in previous tests.[2,3]

C. Debris Distribution

Of the eight tests run, three used simulant corium material. Test #5 had a lower gas flowrate than the other tests. The Wood's metal used as a simulant molten corium material formed a pool on the floor of the cavity and was not entrained at a gas flow of 0.054 kg/s. Of the material that was collected after completion of test #5, ~ 85% of the WM remained in the cavity. The remaining 15% had been dispersed to the weir wall containment section by the initial splashing-type action. Tests #7 and #8 were high gas flowrate tests. Of the WM collected in these tests, ~ 8% remained in the cavity and ~ 92% was swept from the cavity to the weir wall section. The results of these tests, performed with and without water, show that the removal of WM was relatively independent of the presence of water with gas flow exceeding the sweepout threshold of both materials. The water served as a quench and fragmentation medium for the WM in test #8.

IV. ANALYSIS AND DISCUSSION OF RESULTS

A. Basis for Sweepout Model

The photographic records from the dispersal threshold tests show that as the gas jet entered the cavity mock-up from the top, it first caused a crater-like depression in the surface of the water pool. As the flowrate was increased, the crater depth eventually extended to the vessel bottom and grew in the radial direction. The gas jet was redirected upward off the base, and, outside the central zone of the downward jet, there was net upward flow since the exit pathways were located at the upper region of the cavity. The redirected jet caused a stripping-like disengagement of droplets from the water. This initial entrainment was due to *locally* high shear velocity which surpassed the entrainment threshold at the gas/liquid boundary (crater wall). However, the droplets that disengaged typically fell back downward to the water layer. A flowrate was eventually reached when there was no longer a discernable water layer on the bottom, and the entire water mass was essentially fluidized. At this point water droplets began to be carried upward and out the exit ports with the upward flowing gas. Hence, from visual appearance, the water sweepout threshold coincided with the onset of a fluidized state of the water layer.

The minimum superficial gas velocity to cause fluidization of a water layer is given by the expression:[4]

$$U_{g,F} = 0.2 \left[\frac{(\rho_\ell - \rho_g)\, g\sigma}{\rho_g^2} \right]^{1/4} \qquad (1)$$

where ρ_ℓ is the density of the liquid, ρ_g is the density of the gas, g is the acceleration of gravity, and σ is surface tension of the liquid. Strictly speaking, Eq. 1 applies for the case of gas flowing upward from below the water layer, as through a porous plate. Its use in this case constitutes an approximation based upon two observations of the flow regime in the model tests. First, at incipient fluidization, the gas jet penetrates to the base of the vessel and spreads radially on the base causing a significant undercutting and entrainment of the liquid. Second, the upward gas velocity outside

the downward jet region was approximately uniform. Hence a model of uniform upward gas flow from beneath the (partially) fluidized water layer was suggested by the observed flow regime.

B. Model Predictions for Experiments

The gas mass flowrates through the cavity system at the onset of sweepout are listed in Table 1 for the three quasi-static threshold tests performed. The superficial velocity of the gas flowing upward through the cavity mock-up vessel is determined from:

$$U_g = \frac{\dot{M}_t}{\rho_g A_g} \qquad (2)$$

where the upward gas velocity is assumed uniform over an area A_g and A_g is assumed equal to the cross-sectional area of the vessel (286 cm^2) less the cross-sectional area of downward-flowing gas jet. In the experiments the jet diameter at the impingement region of the base was observed to be 2.5 x the nozzle diameter, from which A_g = 254 cm^2 was used in the calculations. The gas was nitrogen at a pressure ~ 0.1 MPa in the vessel (ρ_g = 1.14 x 10^{-3} g/cm^3); $\dot{M}_t$ in Eq. 2 is the measured gas mass flowrate at the onset of significant sweepout. From this simplified model of the experiment flow geometry, the gas superficial velocity at the onset of water sweepout is calculated to be 0.87 m/s for tests 1 and 2 and 1.04 m/s for test 3.

The predicted sweepout threshold based on the fluidization model was calculated using Eq. 1. The parameter values used for the nitrogen/water system were ρ_H = 1 g/cm^3, ρ_L = 1.14 x 10^{-3} g/cm^3, g = 10^3 cm/s^2, and σ = 0.070 N/m. The fluidization threshold is found to occur at a predicted superficial velocity of 0.96 m/s, in very close agreement with the experiment sweepout thresholds. This calculation was also performed for the nitrogen/Wood's metal system using ρ_H = 9.2 g/cm^3, ρ_L = 1.14 x 10^{-3} g/cm^3, g = 10^3 cm/s^2, and σ = 0.5 N/m. The predicted fluidization threshold is calculated to be 2.74 m/s for this case.

C. Model Predictions for Reactor System

The model described in the previous sections has been applied to the full-size reactor system to estimate the thresholds for sweepout of both water and corium. Water may or may not be present in the pedestal region depending upon design and accident scenario details. The molten corium is considered to enter the cavity as a result of meltthru of the vessel lower head to which the corium had drained. The corium is ejected into the cavity through the vessel breach at the prevailing vessel-to-drywell pressure differential. The breach can be expected to increase in size due to ablation of the steel wall by the flowing corium. The case of gravity drainage is considered first (RPV completely depressurized). If water is present on the floor, a quench process will begin, and the steam will flow upward and out of the pedestal region through the available pathways, namely the manway and CRD openings in the pedestal wall. In some cases the steam flow alone may be sufficient to cause substantial depletion of the water inventory by sweepout. If the cavity contains no water, the corium will simply splash off the floor and resettle, forming an accumulation of melt and crust which can be expected to thermally attack the concrete. The gas created by concrete decomposition will flow upward and out the exit pathways, but it is expected to be too little to cause any significant sweepout of the corium.

The principal source of gas flowing through the cavity region occurs for accident sequences involving high RPV pressure. The steam and H_2 break through the corium layer in the bottom head (following the stage of essentially single-phase corium ejection) and initiates a gas blowdown into the cavity. For given vessel and drywell conditions, the principal parameter determining the blowdown flowrate is the breach throat area, A_t. The simplified analysis presented here determines the breach area at which the blowdown flowrate is sufficiently large to cause fluidization and sweepout of water *and/or* corium from the cavity. The augmentation of the system flowrate by steam or gas generated by corium/water and corium/concrete interactions is ignored in this simplified analysis. To include these effects would result in a smaller A_t for sweepout initiation than is calculated here.

The gas blowdown from the vessel is assumed to be essentially single phase, the blowdown gas is assumed to be all steam (the presence of H_2 is

ignored in this simplified analysis), and the vessel-to-drywell pressure difference is such that the discharge is choked at the breach. Under these conditions the blowdown is described by:[1]

$$\frac{\dot{M}_t \sqrt{RT_1}}{C_d A_t p_1} = \sqrt{k \left(\frac{2}{k+1}\right)^{\frac{k+1}{k-1}}} \qquad (3)$$

For steam, $k \simeq 1.3$, and Eq. 3 becomes

$$\frac{\dot{M}_t \sqrt{RT_1}}{C_d A_t p_1} = 0.667 \qquad (4)$$

In Eq. 4, T_1 and p_1 are the steam temperature and pressure conditions in the vessel, R is the gas constant for dry steam, C_d is a discharge coefficient, A_t is the breach area, and $\dot{M}_t$ is the mass discharge rate through the breach. Combining Eqs. 1, 2 and 4 gives a relationship for the minimum breach size resulting in fluidization and sweepout:

$$\frac{A_{t,F}}{A_g} = \frac{0.3 \rho_g \sqrt{RT_1}}{C_d p_1} \left[\frac{(\rho_\ell - \rho_g) g \sigma}{\rho_g^2}\right]^{1/4} \qquad (5)$$

For the specific cases to be calculated, we assume the reactor pressure vessel to contain saturated steam at 7.1 MPa (1000 psi), and we assume that upon blowdown the steam remains saturated at the drywell condition of 0.3 MPa. We neglect steam condensation and we neglect heating effects by corium dispersed in the cavity. Although the area in the cavity available for upward gas flow is less than the total area due to the downward gas jet, we neglect the latter area for simplicity and set $A_g = 33\ m^2$, using the entire cross-sectional area inside the pedestal region. The discharge coefficient C_d is set equal to 0.6 for the vessel breach which is assumed to be circular in cross section, sharp edged, and small in diameter in relation to the vessel cross-sectional area.

The minimum velocity required to cause fluidization of a water layer in the bottom of the cavity is calculated from Eq. 1 to be ~ 0.8 m/s. For the conditions assumed in the RPV and drywell, the breach area needed in the RPV

lower head to produce this superficial efflux velocity is calculated from Eq. 5 to be 78 cm^2, equivalent to a circular hole of 10 cm diameter. In order to fluidize the denser corium (ρ_ℓ = 7.27), a larger fluidization velocity of 2.16 m/s is calculated. This corresponds to a breach area of 214 cm^2, equivalent to a 16.5 cm diameter opening in the vessel lower head.

It is concluded from these scoping-type calculations that sweepout of both water and corium from the pedestal region is possible by a fluidization process resulting from vessel blowdown through a sufficiently large breach in the RPV. Water has a lower threshold for sweepout than corium, namely, ~ 0.8 vs. ~ 2.2 m/s upward superficial gas velocity. The minimum breach sizes for a vessel at 1000 psi to cause flowrates through the cavity exceeding these thresholds are estimated to be ~ 10 and 17 cm diameter, respectively.

V. ACKNOWLEDGEMENT

This work was sponsored by the Atomic Industrial Forum for the Industry Degraded Core Rulemaking (IDCOR) Program. The authors are indebted to R. E. Henry, Fauske and Associates, who served as technical coordinators for this work, and to E. L. Fuller, IDCOR, who served as program manager. Helpful discussions were also held with J. J. Sienicki and L. W. Deitrich, ANL. Figures were drawn by J. Logan. The manuscript was prepared for publication by V. Eustace.

VI. REFERENCES

1. B. W. Spencer, M. Bengis, S. P. Baronowsky, and J. J. Sienicki, "Sweepout Thresholds in Reactor Cavity Interactions," ANL/LWR/SAF 82-1 (1982).

2. B. W. Spencer, D. J. Kilsdonk, and J. J. Sienicki, "Hydrodynamics Aspects of Ex-vessel Debris Dispersal in Zion-type Containment Design," ANL/LWR/SAF 83-1 (1983).

3. Grand Gulf Nuclear Station, Units 1 and 2, Preliminary Safety Analysis Report, Amendment 49 (Includes Final Safety Analysis Report), Mississippi Power and Light Company (1981).

4. G. B. Wallis, One-dimensional Two-phase Flow, McGraw-Hill Book Co., New York, NY (1969).

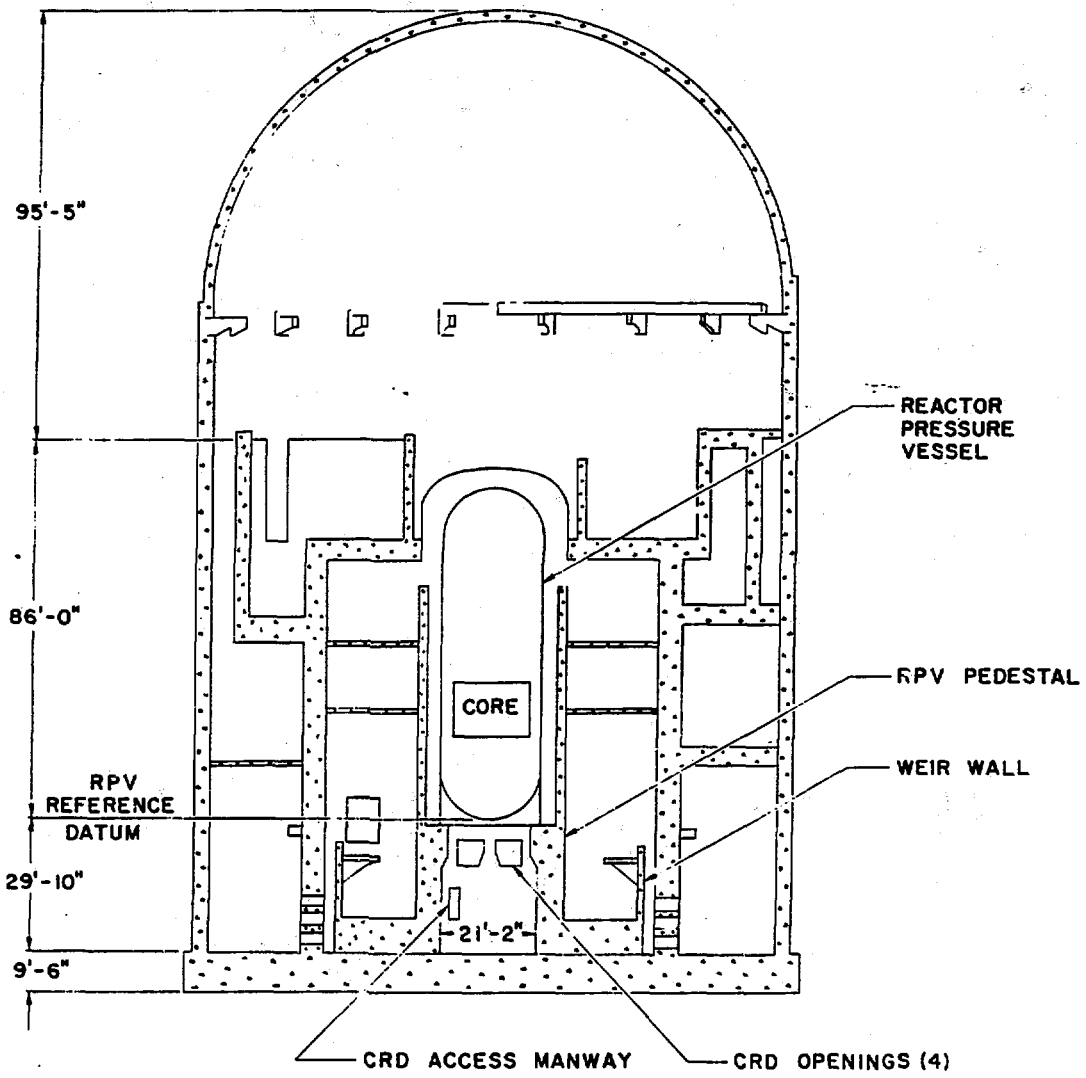

Figure 1. Schematic of Grand Gulf Containment

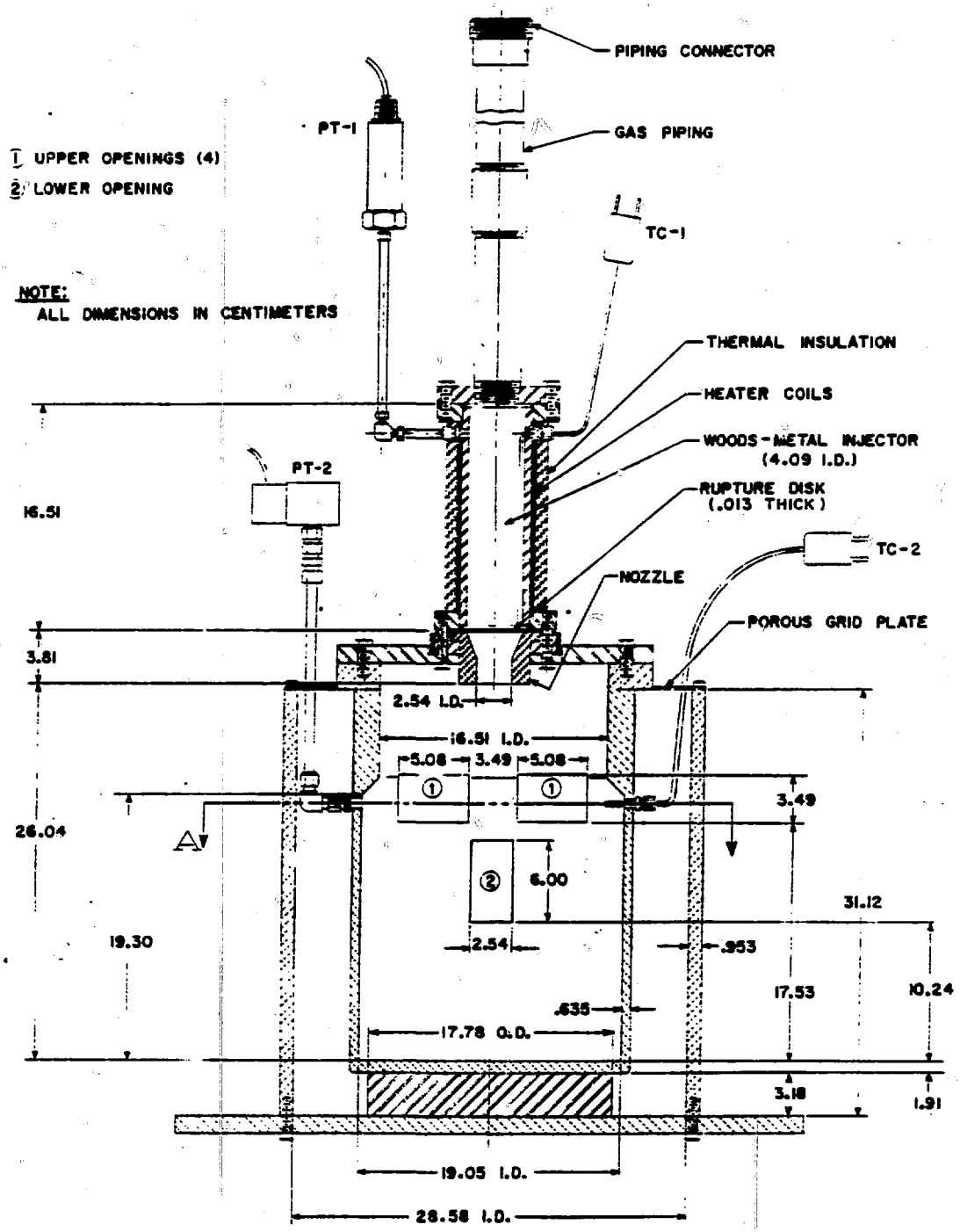

Figure 2a. Schematic of Cavity Mock-up - Side View

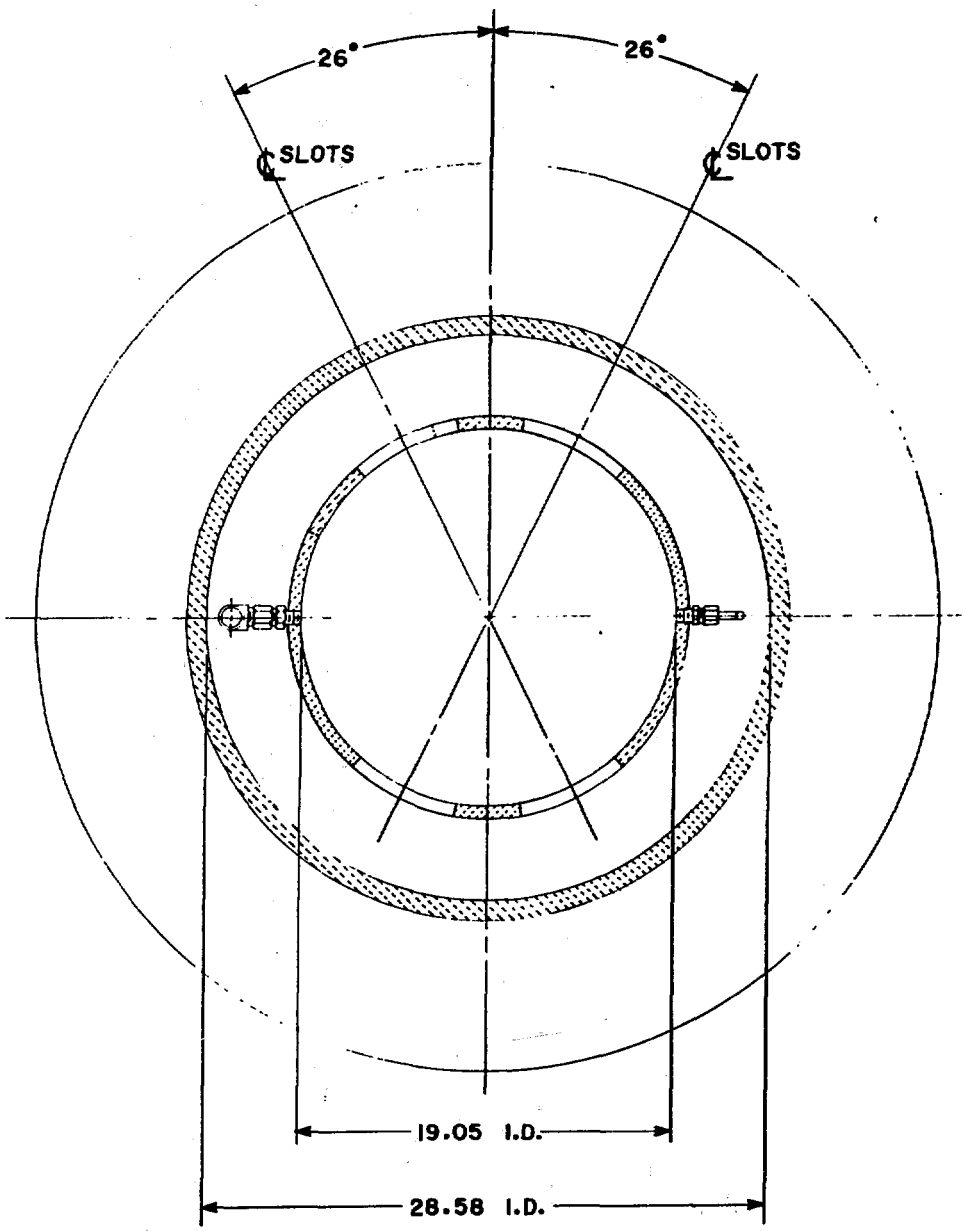

SECTION A=A

Figure 2b. Schematic of Cavity Mock-up - Top View

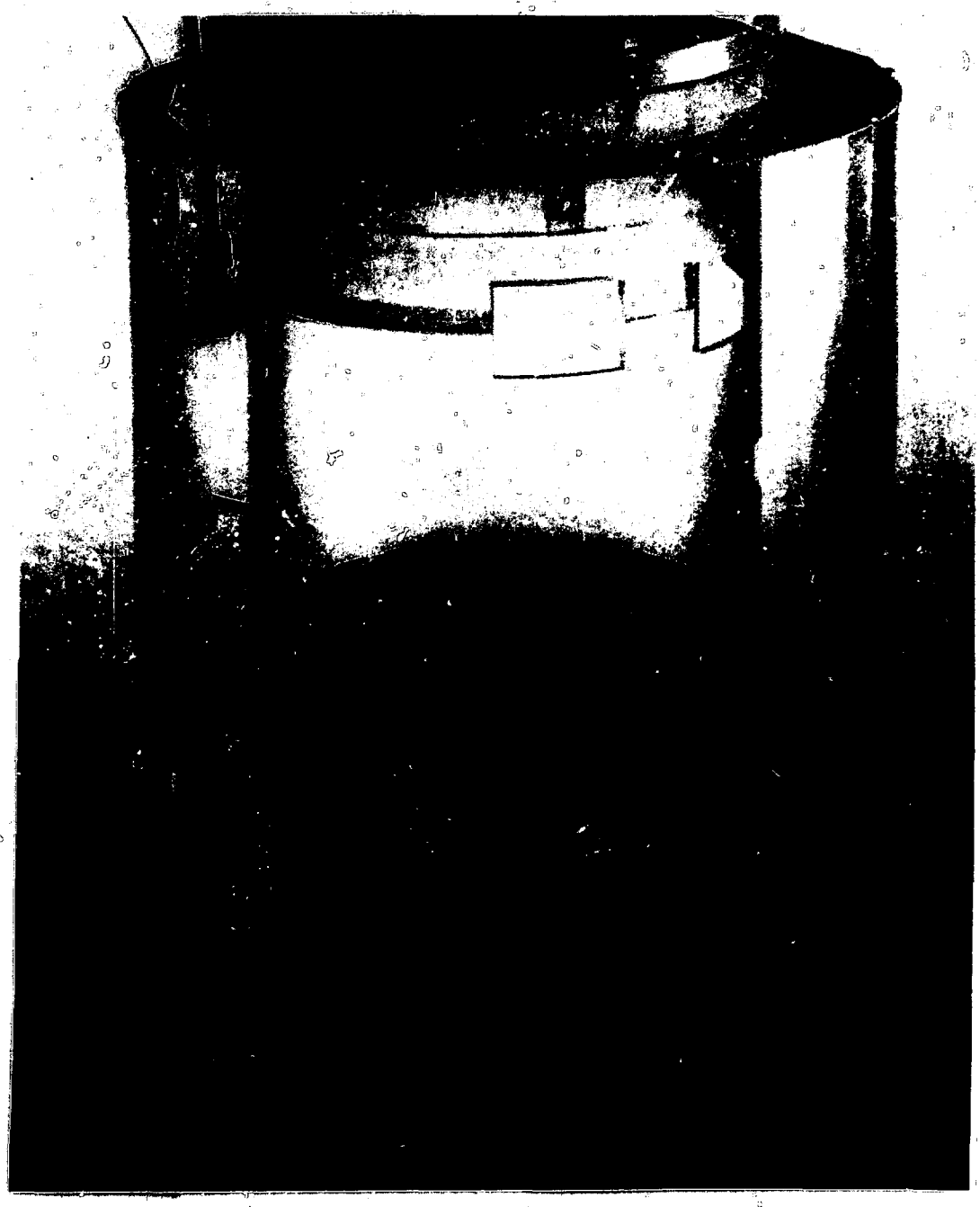

Figure 3. Cavity Mock-up

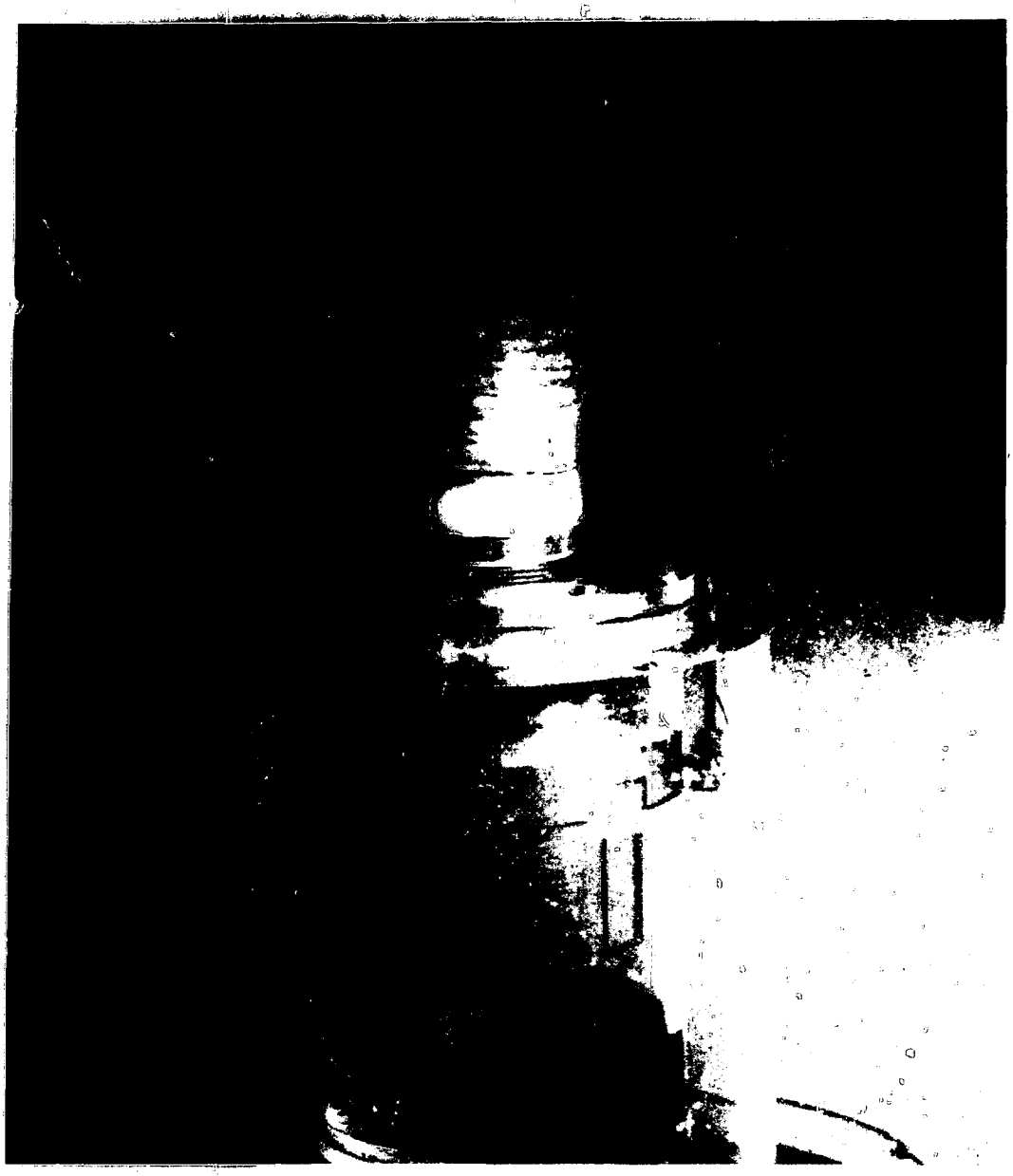

Figure 4. Cavity Mock-up with Wood's Metal Injector

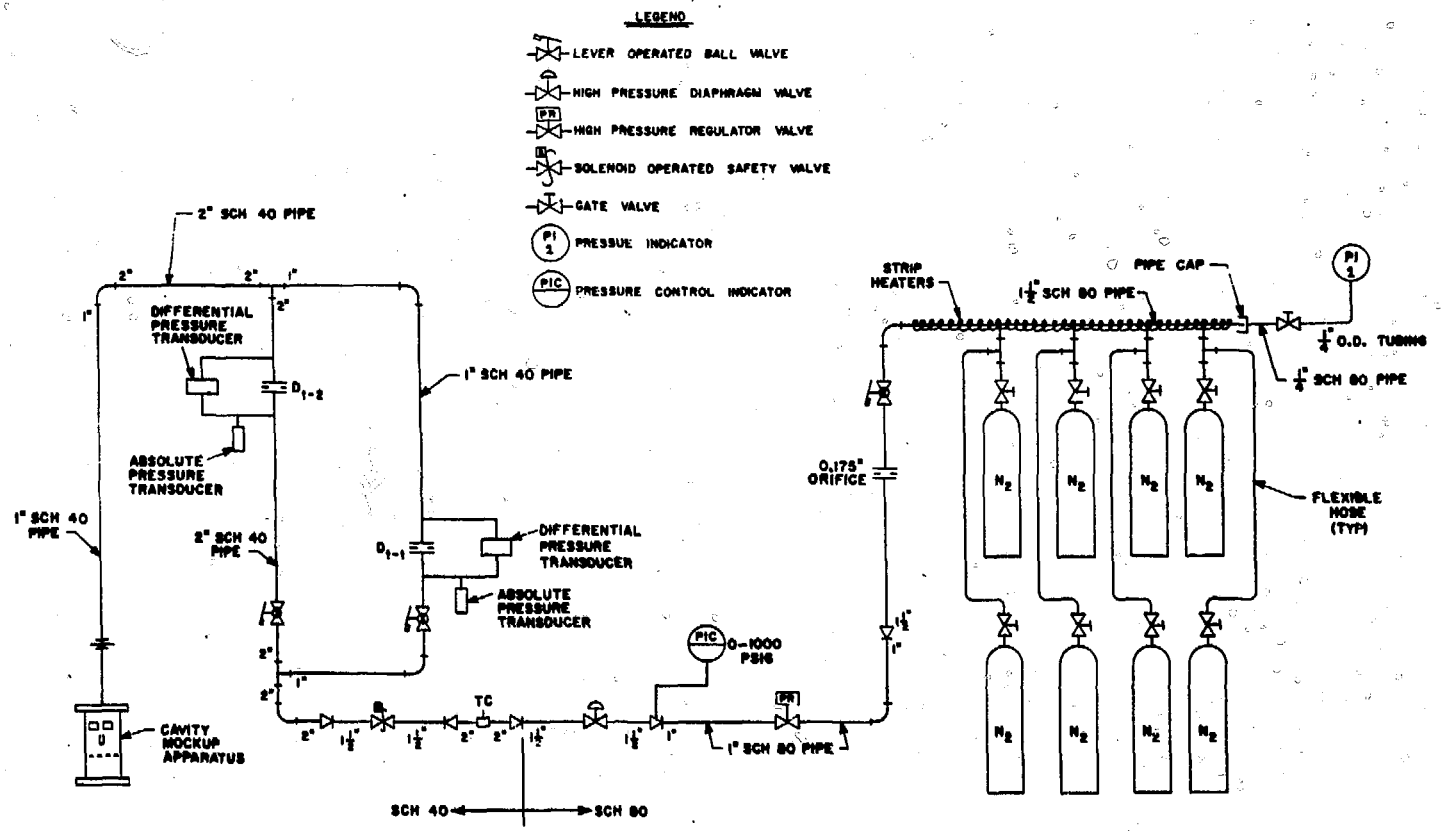

Figure 5. Schematic Illustration of Gas System

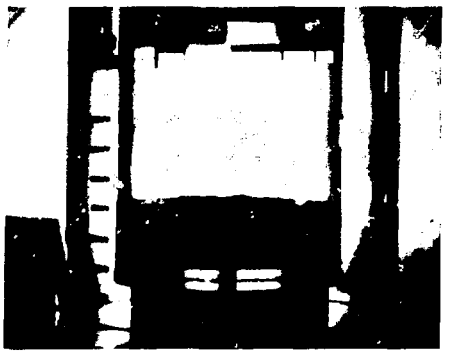

t = 40 ms

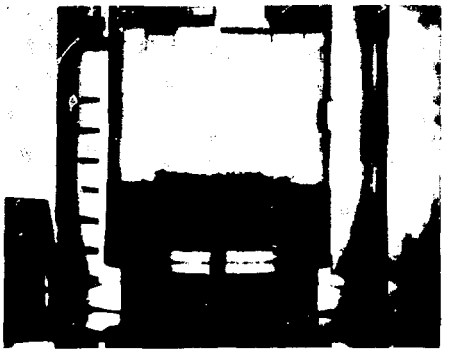

t = 60 ms

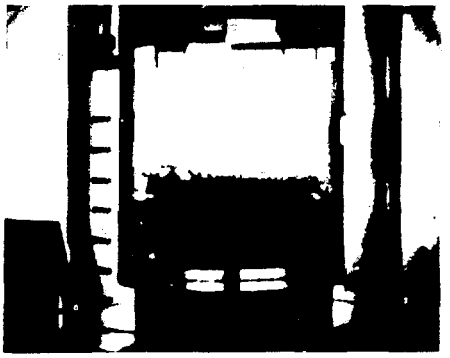

t = 80 ms

t = 120 ms

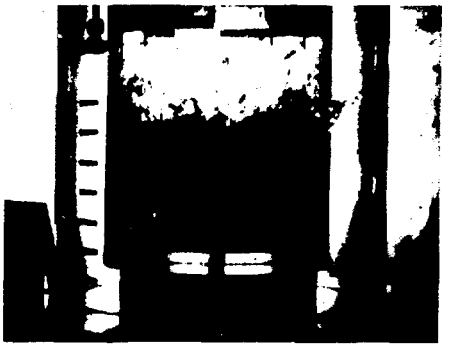

t = 150 ms

t = 240 ms

Figure 6a. Selected Motion Picture Frames from Test #4

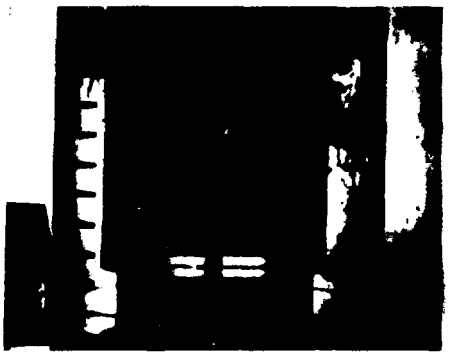

t = 400 ms

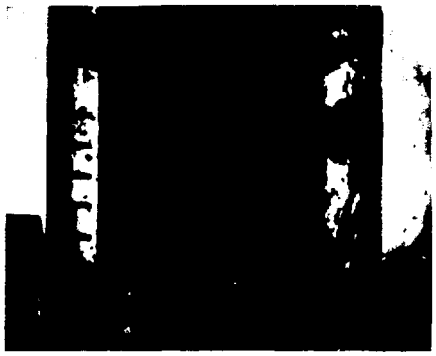

t = 1600 ms

t = 2400 ms

t = 3600 ms

t = 4800 ms

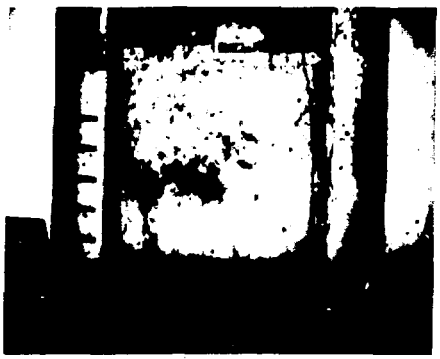

t = 6000 ms

Figure 6b. Selected Motion Picture Frames from Test #4

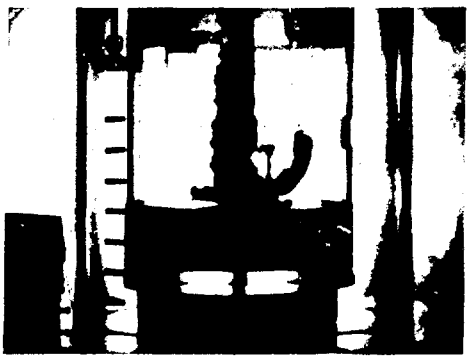

t = 60 ms

t = 70 ms

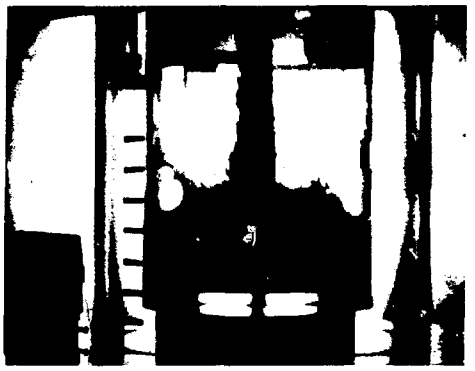

t = 80 ms

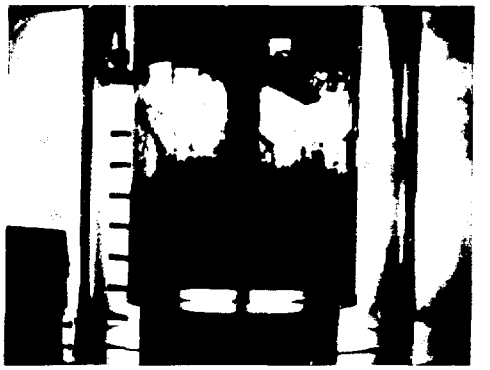

t = 100 ms

Figure 7a. Selected Motion Picture Frames from Test #5

t = 120 ms

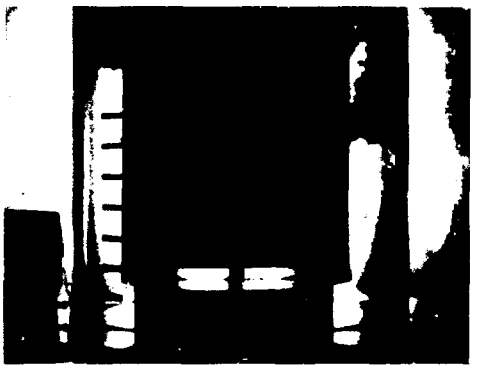

t = 220 ms

t = 1000 ms

t = 4000 ms

Figure 7b. Selected Motion Picture Frames from Test #5

Figure 8. Photo of Cavity after Test #5

Figure 9. Close-up of Debris after Test #5

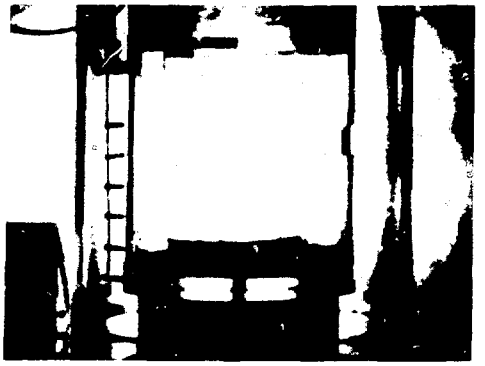

t = 10 ms

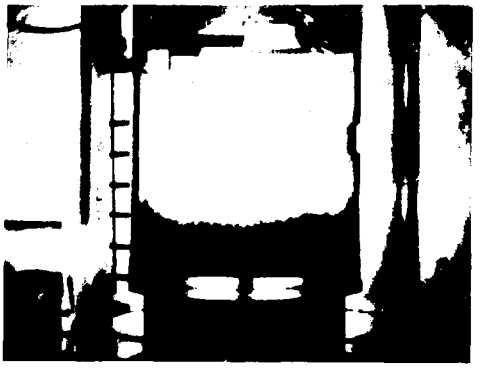

t = 20 ms

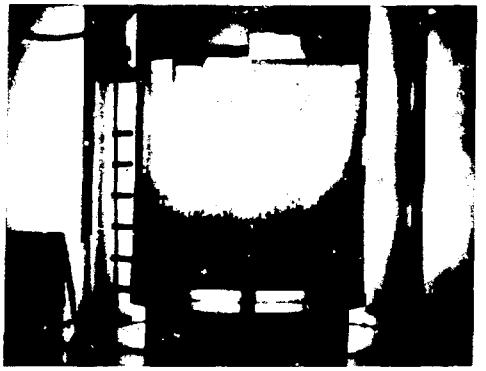

t = 30 ms

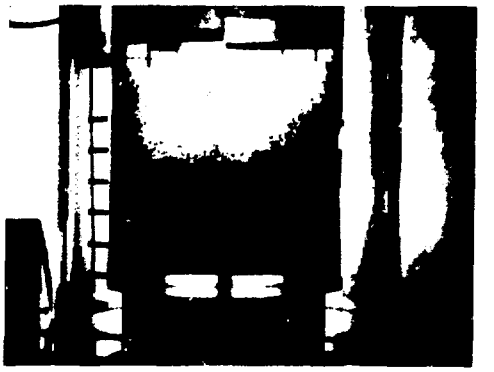

t = 54 ms

Figure 10a. Selected Motion Picture Frames from Test #6

t = 140

t = 200 ms

t = 300 ms

t = 400 ms

Figure 10b. Selected Motion Picture Frames from Test #6

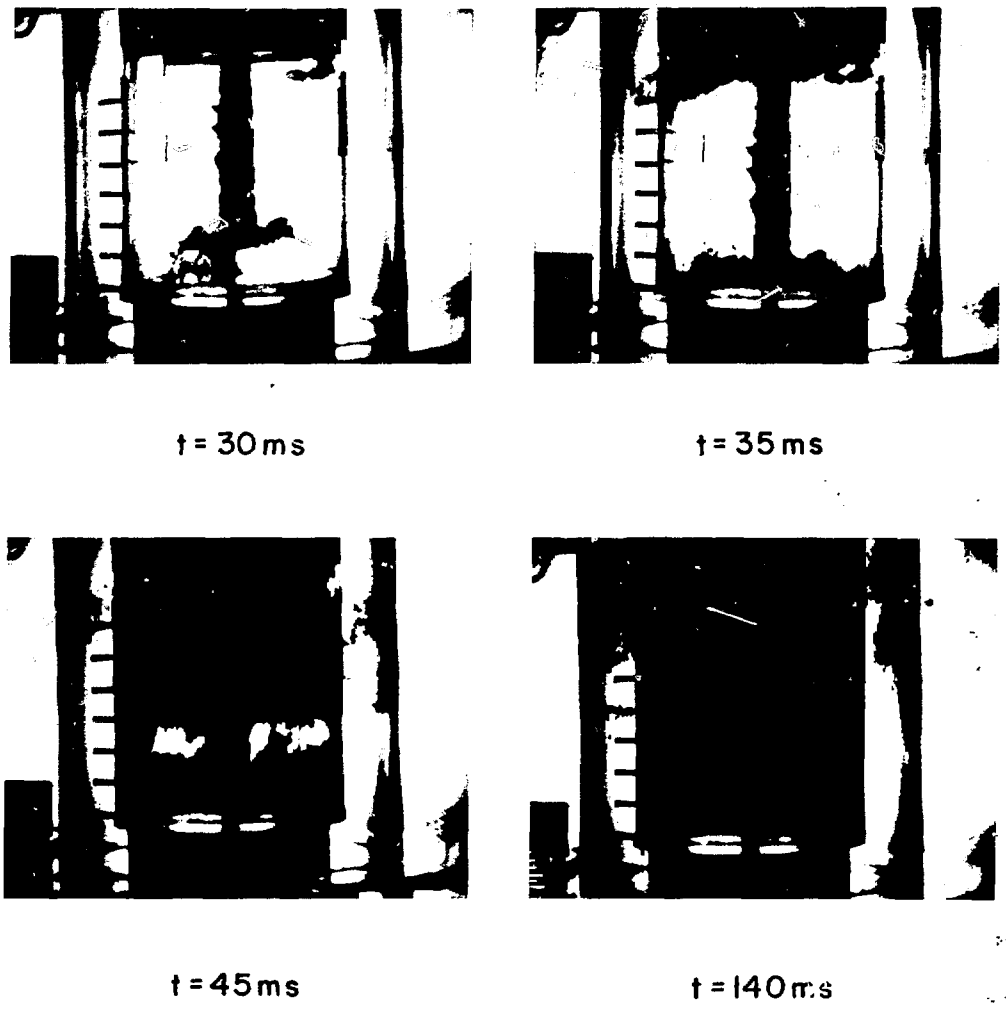

Figure 11a. Selected Motion Picture Frames from Test #7

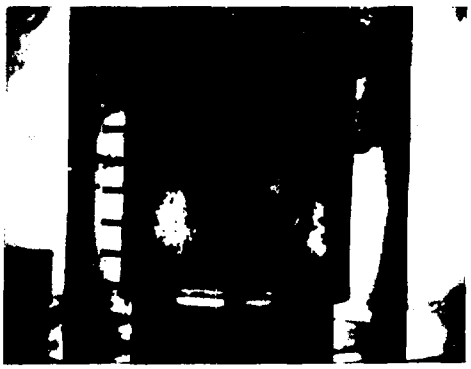

t = 200 ms

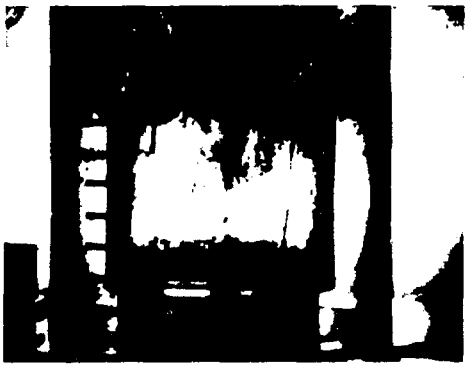

t = 300 ms

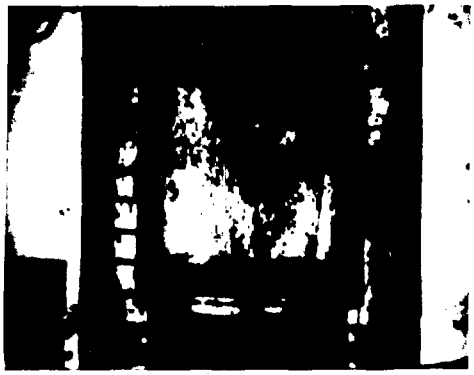

t = 500 ms

t = 900 ms

Figure 11b. Selected Motion Picture Frames from Test #7

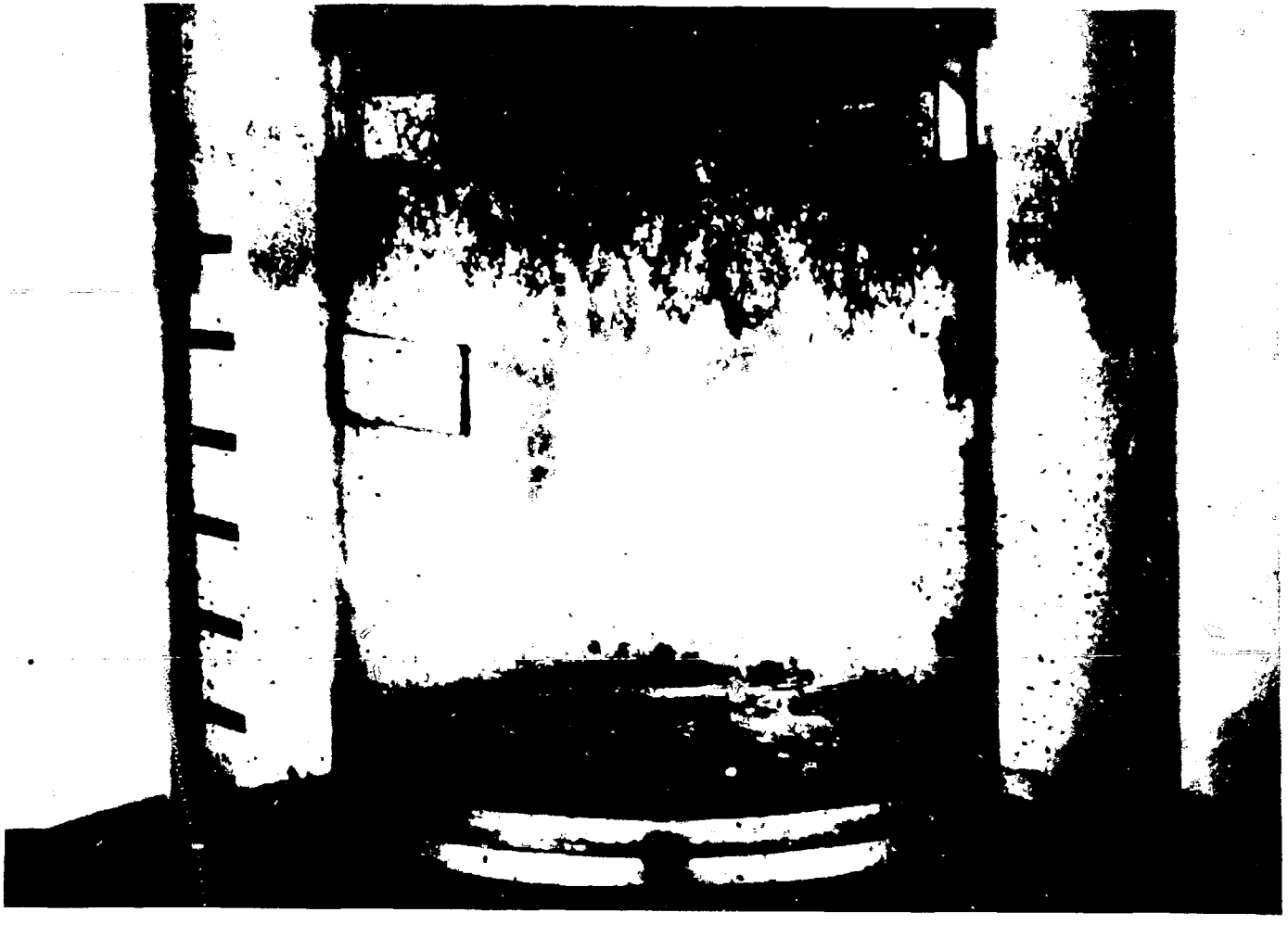

Figure 12. Photo of Cavity after Test #8